Journal of Physical and Theoretical Chemistry
of Islamic Azad University of Iran, 16 (3, 4) 75-90: Fall 2019 & Winter 2020
(J. Phys. Theor. Chem. IAU Iran)
ISSN 1735-2126

Removal of Ni (II) ions from Aqueous Solutions Using Origanum majorana-Capped Silver NanoParticles Synthesis Eequilibrium

Zahra Kazemi[1], Farzaneh Marahel[1]*, Touba Hamoule [2] and Bijan Mombini Godajdar[3]

[1, 2, 3] Department of Chemistry, Omidiyeh Branch, Islamic Azad University, Omidiyeh, Iran

Received December 2019; Accepted January 2020

ABSTRACT

The applicability of Origanum majorana-Capped Silver nanoparticles synthesis for removing Ni (II) ions from aqueous solutions has been reported. This novel material was characterized by different techniques such as FT-IR, XRD and SEM. The influence of nanoparticle dosage, pH of the sample solution, individual ions concentration, temperature, contact time between the sample and the adsorbent were studied by performing a batch adsorption technique. The maximum removal of 30 mg L^{-1} of individual ions from an aqueous sample solution at pH 9.0 for Ni (II) ions was achieved within 60 min when an adsorbent amount of 40 mg for Ni (II) ions was used. It was shown that the adsorption of Ni (II) ions follows the pseudo-second-order rate equation, while the Langmuir model explains equilibrium data. Isotherms had also been used to obtain the thermodynamic parameters such as free energy (ΔG^0), enthalpy (ΔH^0) and entropy (ΔS^0) of adsorption. The negative value of (ΔG^o, ΔH^o and ΔS^o) confirmed the sorption process was endothermic reflects the affinity of origanum majorana-capped silver nanoparticles synthesis for removing Ni (II) ions. A maximum adsorption capacity in binary-component system (180.0 mg/g for Ni (II) ions).

Keywords: Adsorption; Ni(II) ions, Origanum majorana-Capped Silver nanoparticles, Isotherms; Thermodynamic

1. INTRODUCTION

Many concerns about heavy metals contaminating our wastewater rise nowadays and discharge a large amount of metal-contaminated wastewater usually come from industries, commercial, and domestic areas. Generally, wastewaters generated from industrial and domestic consist of Several types of heavy metals such as nickel, cadmium, chromium, cuprum, lead, and zinc, which allare most hazardous from the chemical-intensive industries. It is due to their high solubility in aquatic environments that heavy metals can be absorbed by living organisms. Once they enter the food chain, large concentrations of heavy metals may accumulate in the human body. If the metals concentrations are ingested beyond

*Corresponding author: Farzane.marahel.fm@gmail.com

the permitted value, they can cause serious health disorders. Heavy metal removal from inorganic effluent can be achieved by conventional treatment processes such as chemical precipitation, ion exchange, and electrochemical removal. These processes have significant disadvantages, including complex equipment, high energy consumption, and the generation of toxic sludge [1,2]. Nickel, as a hazardous heavy metal is found in various industrial activities like nickel plating, colored ceramics, batteries, furnaces used to make alloys or from power plants and trash incinerators. Over-absorption of nickel may cause cancer of lungs, nose and bones, extreme weakness, dermatitis, headache, dizziness and respiratory distress [3].

Therefore, removal of these heavy metal ions from such industrial effluents is challenging requirement to produce a safe and clean environment. Many technologies have been developed for removal of heavy metal ions from aquatic environments, including chemical precipitation, chemical oxidation/reduction, reverse osmosis, ion exchange, electro dialysis, ultra-filtration and adsorption [4,5]. Among them, the wide application of adsorption is emerged from advantages including simplicity, low cost, high efficiency, wide adaptability and availability of different adsorbents[6].

Adsorption is one of the best and simple techniques for the removal of toxic and noxious impurities in comparison to other conventional protocols like chemical coagulation, ion exchange, electrolysis, biological treatments is related to advantages viz. lower waste, higher efficiency and simple and mild operational conditions. Adsorption techniques also have more efficiency in the removal of pollutants which are highly stable in biological degradation process through economically feasible mild pathways [7,8]. Hence, nanomaterial's based adsorbents it has been extensively used for removal of different chemicals from aqueous solutions [9]. The efficient applicability of an adsorption process mainly depends on the physical and chemical characteristics of the adsorbent, which is expected to have high adsorption capacity and to be recoverable and available at economical cost. Currently, various potential adsorbents have been implemented for removal of specific organics from water samples. In this regard, magnetic nanoparticles (MNPs) have been studied extensively as novel adsorbents with large surface area, high adsorption capacity and small diffusion resistance. For instance, they have been used for separation of chemical species such as environmental pollutants, metals, dyes, and gases [10].

Nanotechnology is a principally attractive area of research related to producing nanoparticles with various sizes, shapes, chemical compositions, dispersity, and possible application for benefit of human beings [11]. One of the most important fields of research in nanotechnology is the synthesis of different nanoparticles such as silver, gold, iron, and etc [12]. An important area of research in nanotechnology is the synthesis of nano silver particles. Silver has long been recognized as having an inhibitory effect to wards many bacterial strains and microorganisms [13]. Because of their wide range of applications Synthesis of silver nanoparticles is of much interest to the researcher. Generally, nanoparticles are prepared by a variety of chemical and physical methods which are quite expensive and potentially hazardous to the environment which nvolve use of toxic chemicals that are responsible for various biological risks. In the search of cheaper and ecocompatible pathways for nanoparticles, scientist used microorganism [14] and plant extracts [15]. Green synthesis of nanoparticles has

proven to be better methods due to slower kinetics, offer better manipulation, control over crystal growth and their stabilization. Greener synthesis provides advancement over traditionally used nanoparticles synthesis methods chemical [16]. or large scale synthesis and in this method there is no need to use toxic chemicals. Green synthesis of nanoparticles is a bottom up approach where the main reaction occurring is reduction. Biogenic synthesis is useful not only because of its reduced environmental impact [17]. The surface stabilization and functionalization of AgNPs is essential in sensing for metal ions [18].

In this work, origanum majorana-capped AgNPs as a novel adsorbent followed by the characterization using different techniques such as Fourier transform infrared spectroscopy (FTIR), X-ray diffraction (XRD) and scanning electron microscopy (SEM). This adsorbent was used for the ultrasound-assisted removal of Ni(II) ions from aqueous solutions[19]. Therefore, we were motivated to prepare origanum majorana-capped AgNPs as an alternative to expensive or toxic adsorbents for the removal of Ni(II) ions from wastewater. The experimental conditions, such as pH of solution, contact time, initial ions concentration, and adsorbent dosage as well as the dyes removal percentage as response, were studied and optimized. Various isotherm models, such as Langmuir, Freundlich, Tempkin, and Dubinin–Radushkevich were used to fit the experimental equilibrium data. The results showed the suitability and applicability of the Langmuir model. Kinetic models, such as pseudo-first-order, pseudo-second-order diffusion models indicated that the pseudo-second-order model controls the kinetic of adsorption process. It was shown that the origanum majorana-capped AgNPs can be effectively used to remove the heavy metals of Ni(II) ions from wastewater.

2. EXPERIMENTAL

2-1. Instrumentation

Atomic Absorption Spectrophotometer "Shimadzu 6800" equipped with an air-acetylene flame. At room temperature. Fourier transform infrared (FT-IR) spectra were recorded on a PerkinElmer (FT-IR spectrum BX, Germany). The morphology of samples was studied by scanning electron microscopy (SEM: KYKY-EM 3200, Hitachi Company, China) under an acceleration voltage of 26kV).Transmission electron microscopy (TEM) images were taken on a JEOL 3010. The pH/Ion meter (model-728, Metrohm Company, Switzerland, Swiss) was used for the pH measurements. Laboratory glassware was kept overnight in 10% nitric acid solution. A NBE ultrathermostat (VEB Prufgerate - Werk Medingen, Germany) was used to control the temperature.

2.2. Reagents and materials

All chemicals, Silver nitrate ($AgNO_3$), sodium hydroxide, hydrochloric acid, from Merck Company, Ni (II) ions, and methanol were purchased from Merck Company, solution (Merck, Darmstadt, Germany). The solutions were prepared with doubly distilled water.

2-3. Synthesis of Origanum majorana-Capped Ag NPs

Silver nanomaterials of varying sizes and shapes have been utilized in a broad range of applications and medical equipment, such as electronic devices, paints, coatings, soaps, detergents [20]. Specific physical, optical, and chemical properties of silver nanomaterials are, therefore, crucial factors in optimizing their use in these applications. In this

regard, the following details of the materials are important to consider in their synthesis: surface property, size distribution, apparent morphology, particle composition, dissolution rate.

Origanum majorana-Capped Ag NPs were prepared by the reduction of $AgNO_3$ with $NaBH_4$ as a modifier according to the method in the literature [21]. Briefly, 10.0 mL of origanum majorana (0.1 mM) solution was added into the reaction flask that contained 90.0 mL of $AgNO_3$ (0.1 mM) solution under vigorous stirring. After 15 min was UV–visible spectrum of origanum majorana-capped Ag NPs. Inset picture show origanum majorana-capped Ag NPs. added into the above solution at room temperature and stirred for 1 h. The dark colloidal solution color was changed to bright yellow, confirming that the formation of origanum majorana-capped Ag NPs. The origanum majorana-capped Ag NPs solution was stored in the dark at 4.0 ± 2.0◦C to remain stable for several weeks.

2.4. Adsorption of Ni(II) ions onto Origanum majorana-Capped Ag NPs.

A batch process using origanum majorana-capped AgNPs in presence of ultrasound was applied for binary adsorption of Ni(II) ions, while all experiments were under taken in a cylindrical glass vessel by adding 0.05 g of adsorbent to 10 ml of PH 9.0 for Ni(II) ions as optimum value. The vessel was immersed in an ultrasonic bath for 60 min at room temperature and subsequently the solutions were centrifuged. Then non-adsorbed ions contents were determined by using Atomic Absorption Spectrophotometer Shimadzu 6800 equipped with an air-acetylene flame for Ni(II) ions, respectively.

2.5. Batch adsorption Ni(II) ions adsorption process

Batch adsorption experiments were carried out to determine the Ni(II) ions adsorption isotherm onto origanum majorana-capped AgNPs composite and its thermodynamic properties: 100 mL solution having 100 mg/L concentration of Ni(II) ions was prepared and Initial pH of the solution was adjusted with the help of 0.01N HCl / 0.01N NaOH aqueous solution

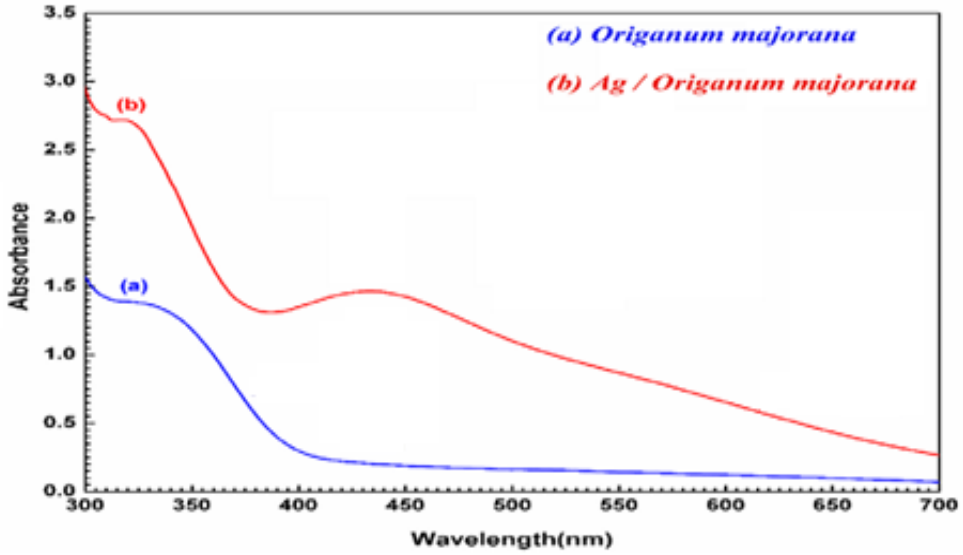

Fig. 1. The absorption spectra of product origanum majorana-capped Ag NPs.

without any further adjustments during the experiments. 10 samples of 50 mL solution were taken in ten 100 mL flasks containing fixed adsorbent dose of 30 mg/L. These flasks were agitated at a constant rate of 200 rpm in a temperature controlled orbital shaker maintained at 25^{oC} temperatures. One of the sample flasks was withdrawn from orbital shaker after fixed time intervals (10, 20, 30, 40, 50, 60, 70 and 80 min) and analyzed for remaining metal ions present in the adsorbate solution. origanum majorana-capped AgNPs was separated from aqueous solution by filtration through Whatman No. 42 filter paper. The Ni(II) ions concentration in solution samples was carried out using a "Shimadzu 6800 Atomic Absorption Spectrophotometer" equipped with an air-acetylene flame. The estimation of metal elimination (%A) or elimination efficiency of metal ions was done using the following equation:

$$R\% = \frac{C_{0i} - C_{ei}}{C_{0i}} \times 100 \quad (1)$$

In the above formula C_0 stands for the initial concentration of Ni(II) ions in solution(mg/L),and C_e stands for the final concentration of Ni(II) ions in solution(mg/L). The calculation of the amount (mg/g) of Ni(II) ions adsorbed at equilibrium was done using the ensuing equation:

$$q_e = \frac{(C_\circ - C_e)V}{W} \quad (2)$$

where $C_\circ(mgL^{-1})$ and $C_e(mgL^{-1})$ are the initial ions concentration and equilibrium ions concentration in aqueous solution, respectively, V (L) is the solution volume and W (g) is the adsorbent mass.

3. RESULTS AND DISCUSSION

3.1. Characterization of adsorbent

The FTIR spectrum of majorana-capped Ag NPs nanoparticles loaded on activated carbon (Fig. 2.a), The broad peaks at ≤900 and 1048 in Ag – O, 1386-1422 cm^{-1} could be assigned to C–H stretching from majorana-capped Ag NPs, and 1634cm^{-1} to C=O bonds. The new peak appearing at 2027 cm^{-1} corresponds to C–H stretching new peak appearing at 3412 cm^{-1} corresponds to – OH stretching [22]. The XRD pattern of the majorana-capped Ag NPs (Fig.2.b) represents a peak at 38.07 (111), 44.26 (200), 64.43 (220) and 77.35 (311) correspond to diffractions and reflections from the carbon atoms [23] As seen, the highly crystalline nature of the after functionalizing with majorana-capped Ag NPs is confirmed, while the high intensity of peak at 38.07 (111) shows that there has been a small amount of material in amorphous state. The observed XRD pattern indicates that the prepared majorana-capped Ag NPs is well-synthesized. The morphological features of the samples studied by SEM are shown in Fig.3). majorana-capped Ag NPs are observed to be smooth, homogeneous, tidy and approximately uniform in size distribution (Fig.3). Afer the surface modification with majorana-capped Ag NPs became rough, larger and bundled [24].

3.2. Effect of pH on metal ion biosorption

The pH has been identified as one of the most important parameter that is effective on dyes sorption. The effect of pH on the Ni(II) ions onto origanum majorana-capped AgNPs was studied at pH 3.0–10.0, Fig.4. The maximum biosorption was observed at pH 9.0 for Ni(II)ions. Therefore, the remaining all biosorption experiments were carried out at this pH value. The biosorption mechanisms on the origanum majorana-capped AgNPs surface reflect the nature of the physic chemical interaction of the solution [25,26]. At highly acidic pH, the overall surface charge on the active sites became. positive

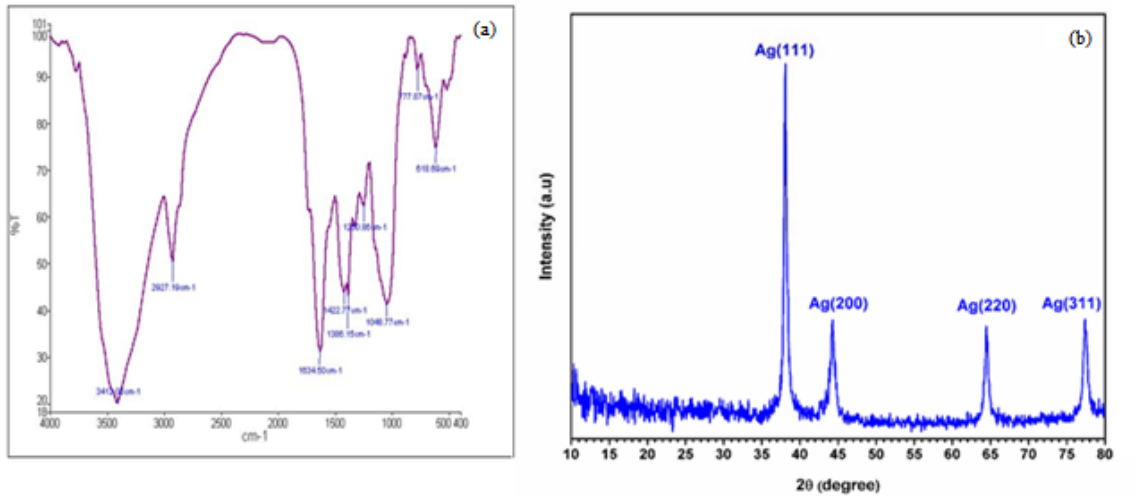

Fig. 2. The (a) FT-IR and (b) XRD image of the prepared majorana-capped Ag NPs.

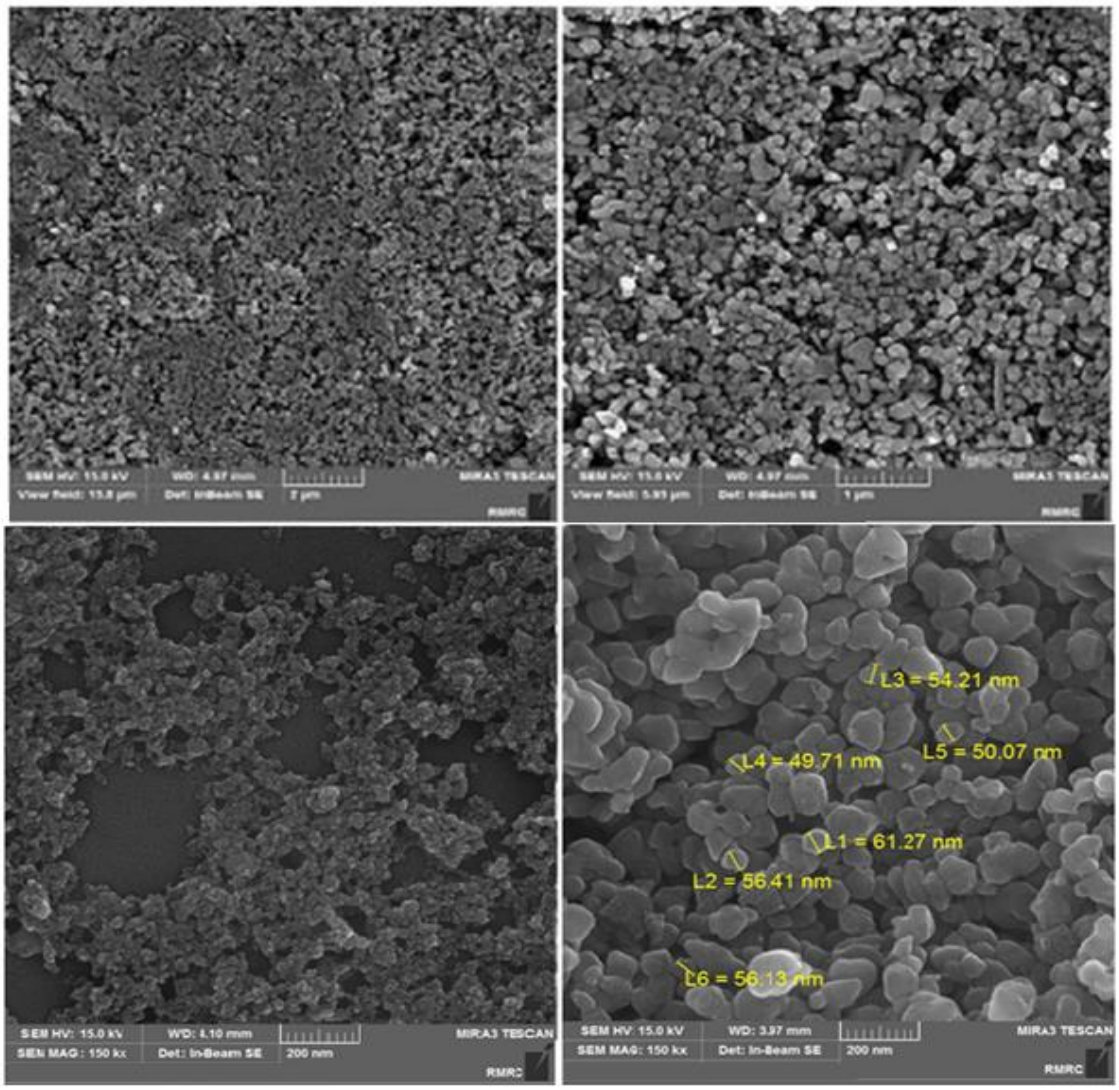

Fig. 3. The (SEM) image of the prepared majorana-capped Ag NPs.

and Ni(II) ions and protons compete for binding sites on origanum majorana-capped AgNPs, which results in lower uptake of Ni(II) ions. The biosorbent surface was more negatively charged as the pH solution increased from pH 9.0 for Ni(II) ions. The functional groups of the origanum majorana-capped AgNPs was more deprotonated and thus available for the Ni(II) ions. Decrease in biosorption yield at higher pH=9 for the Ni(II) ions is not only related to the formation of soluble hydroxylated complexes of the Ni(II), but also to the ionized nature of the origanum majorana-capped AgNPs of the biosorbent under the studied pH. Previous studies also reported that the maximum biosorption efficiency of Ni(II) ions on biomass was observed at pH (9.0).

3.3. Effect of Biosorbent Dose

The biosorbent dosage is an important parameter because this determines the capacity of a biosorbent for a given initial ions concentration. The biosorption efficiency for Ni(II) ions as a function of biosorbent dosage was investigated. The percentage of the metal biosorption steeply increases with the biosorbent loading up to 40 mg Fig.5. This result can be explained by the fact that the biosorption sites remain unsaturated during the biosorption reaction, whereas the number of sites available for biosorption site increases by increasing the biosorbent dose [27]. The maximum biosorption was attained at biosorbent dosage, 40 mg. Therefore, the optimum biosorbent dosage was taken as 5mg for further experiments. This can be explained by when the biosorbent ratio is small, the active sites for binding metal ions on the surface of origanum majorana-capped AgNPs is less, so the biosorption efficiency is low. As the biosorbent dose increased, more active sites to bind Ni(II) ions, thus it results an increase in the biosorption efficiency until saturation.

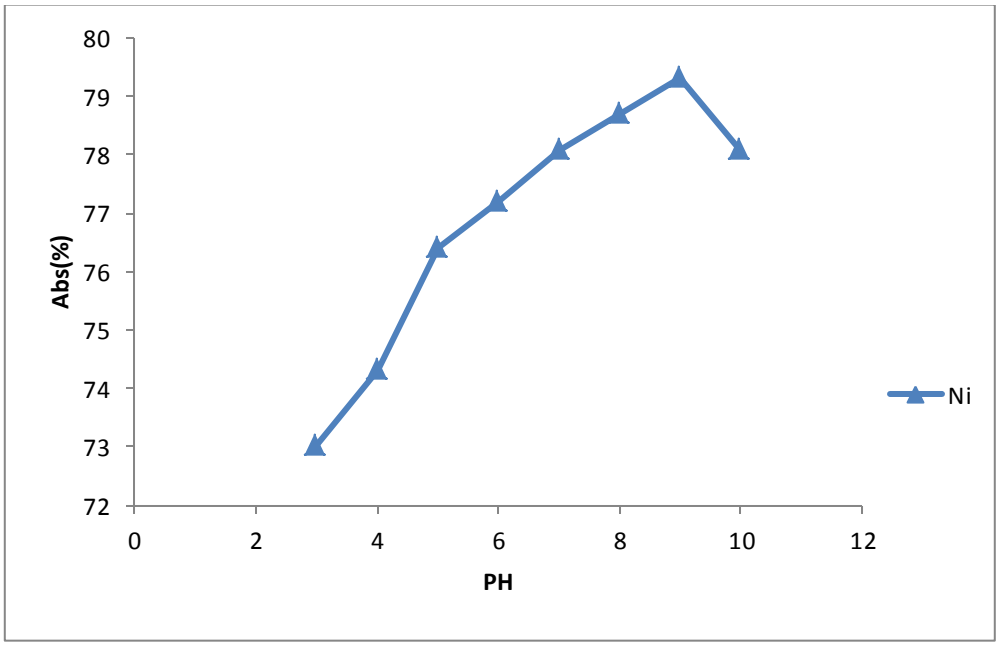

Fig. 4. Effect of initial solution pH on the adsorption amount of Ni(II) ions onto origanum majorana-capped AgNPs.

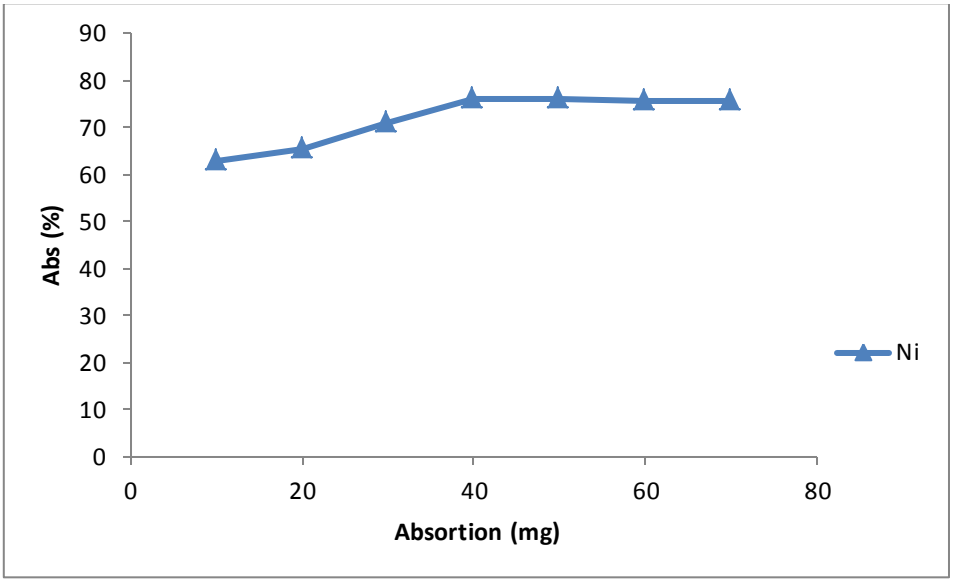

Fig. 5. Effect of dosage origanum majorana-capped AgNPs on the adsorption amount of Ni(II) ions.

3.4. Effect of contact time

The effect of contact time on the adsorption capacity of Ni(II) ions onto origanum majorana-capped AgNPs is shown in fig.6, When the initial Ni(II) ions concentration is increased from 30 mg/L the amount of Ni(II) ions adsorbed onto origanum majorana-capped AgNPs, 10 at 80 min contact time, pH value 9 for Ni(II) ions, 40 mg Ni(II) ions adsorbent dose and the constant temperature 298.15 K. The increase of loading capacity of origanum majorana-capped AgNPs with increasing initial ions concentration may be due to higher interaction between Ni(II) ions and adsorbent [28]. These results show that rapid increase in adsorbed amount of Ni(II) ions is achieved during the first 60 minutes. Similar results were reported before for removal of hazardous contaminants from wastewater.

3.5. Effect of temperature

To study the effects of temperature on the adsorption of Ni (II) ions by origanum majorana-capped AgNPs, the experiments were performed at temperatures from 298.15 to 328.15 K. Fig.7. shows the influence of temperature on the adsorption of ions on origanum majorana-capped AgNPs. As it was observed, the equilibrium adsorption capacity of Ni (II) ions onto origanum majorana-capped AgNPs was found to increase with increasing temperature. This fact indicates that the mobility of Ni (II) ions increased with the temperature, additionally the viscosity of ions solution reduces with rise in temperature and as a result, it increases the rate of diffusion of ions molecules. The results were in agreement with the effect of the solution pH, and temperature on adsorption behavior of reactive Ni (II) ions on activated carbon [29].

3.6. Biosorption Isotherms

An adsorption isotherm describes the fraction of sorbate molecules that are partitioned between liquid and solid phases at equilibrium. Adsorption of Ni (II) ions onto origanum majorana-capped AgNPs was modeled using four adsorption isotherms: Langmuir, Freundlich, Temkin, and Dubinin - Radushkevich isotherms.

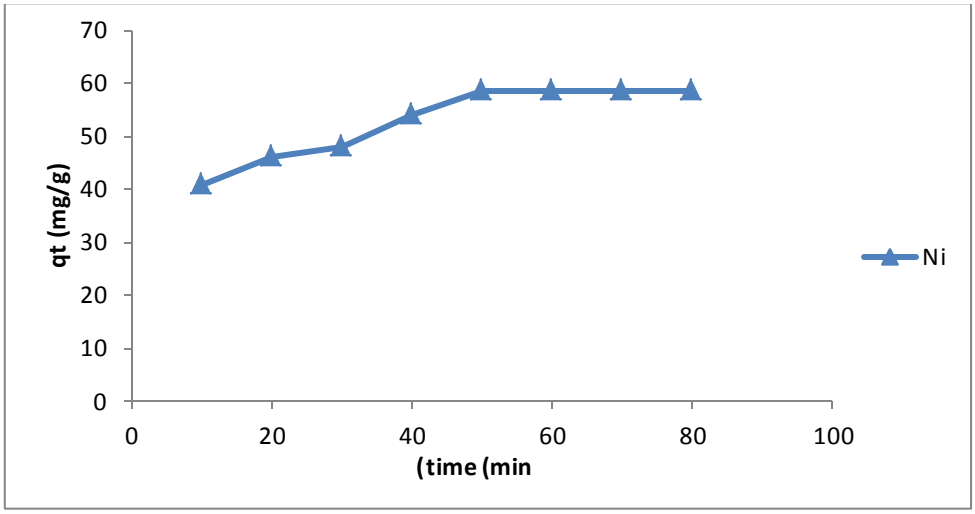

Fig. 6. Effect of contact time on the adsorption of Ni (II) ions by origanum majorana-capped AgNPs.

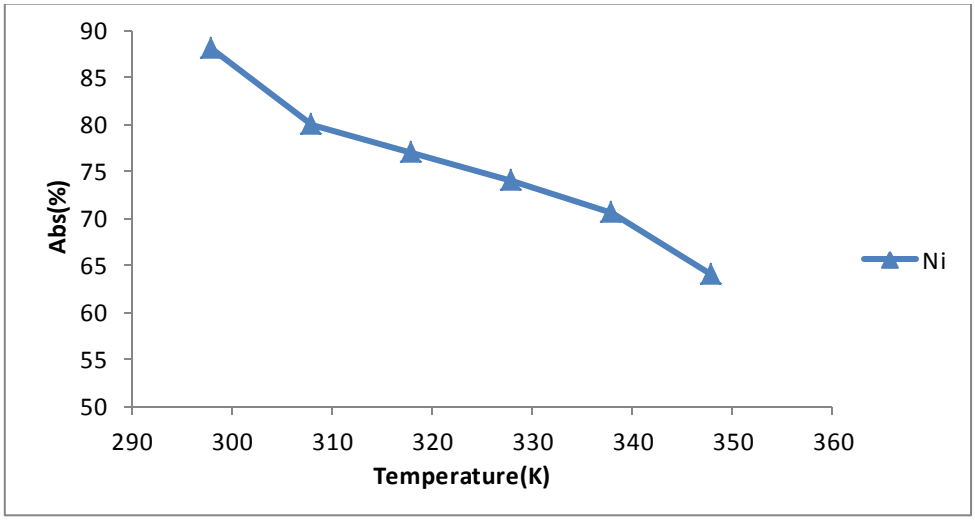

Fig. 7. Effect of temperature on the adsorption amount of Ni (II) ions on origanum majorana-capped AgNPs.

3.7. Adsorption Equilibrium Study

Adsorption equilibrium isotherm is designed based on mathematical relation of the amount of adsorbed target per gram of adsorbent (q_e(mg/g)) to the equilibrium non-adsorbed amount of ions in solution (C_e (mg/L) at fixed temperature [30, 31]. Isotherm studies are divided to well-known models such as Langmuir, Freundlich, Temkin and Dubinin–Radushkevich based on well-known conditions. The Langmuir model is the most frequently employed model given by following equation [32]:

$$q_e = \frac{Q_m K_l C_e}{1+ K_l C_e} \quad (3)$$

where C_e, Q_m and K_L are the concentration of adsorbate at equilibrium (mg/L), maximum monolayer adsorption capacity (mg/g) and Langmuir constant (L/mg), respectively. C_e/q_e was plotted against C_e where parameters such as Q_m, K_L, and R^2 were calculated based on the slope and

intercept of such lines and displayed in Table1. The values of K_a (the Langmuir adsorption constant (L/mg)) and Q_m (theoretical maximum adsorption capacity (mg/g)) were obtained from the intercept and slope of the plot of C_e/q_e versus C_e, respectively. The applicability of Langmuir model for the interpretation of the experimental data over the whole concentration range is proven from high correlation coefficient at all adsorbent masses. The increase in the amount of adsorbent leads to significant enhancement in the actual amount of adsorbed ions. The parameters of Freundlich isotherm model such as K_F and the capacity of the adsorption were calculated from the intercept and slope of the linear plot of $\ln q_e$ versus $\ln C_e$, respectively. The heat of the adsorption and the adsorbent–adsorbate interaction were evaluated by using Temkin isotherm model. In this model, B is the Temkin constan t related to heat of the adsorption (J/mol), T is the absolute temperature(K), R is the universal gas constant(8.314J/mol. K) and K is the equilibrium binding constant(L/mg). D–R model was applied to estimate the porosity apparent free energy and the characteristic of adsorption [33,34]. In this model B (mol^2/kj^2) is a constant related to the adsorption energy, Q_s(mg/g) is the theoretical saturation capacity and E is the Polanyi potential. The slope of the plot of $\ln q_e$ versus ε^2 gives B and its intercept yields the Q_s value. The linear fit between the plot of C_e/q_e versus C_e and calculated correlation coefficient (R^2) for Langmuir isotherm model shows that the ions removal isotherm can be better represented by Langmuir model (Table 1). This confirms that the adsorption of ions takes place at specific homogeneous sites as a monolayer on to the origanum majorana-capped AgNPs surface.

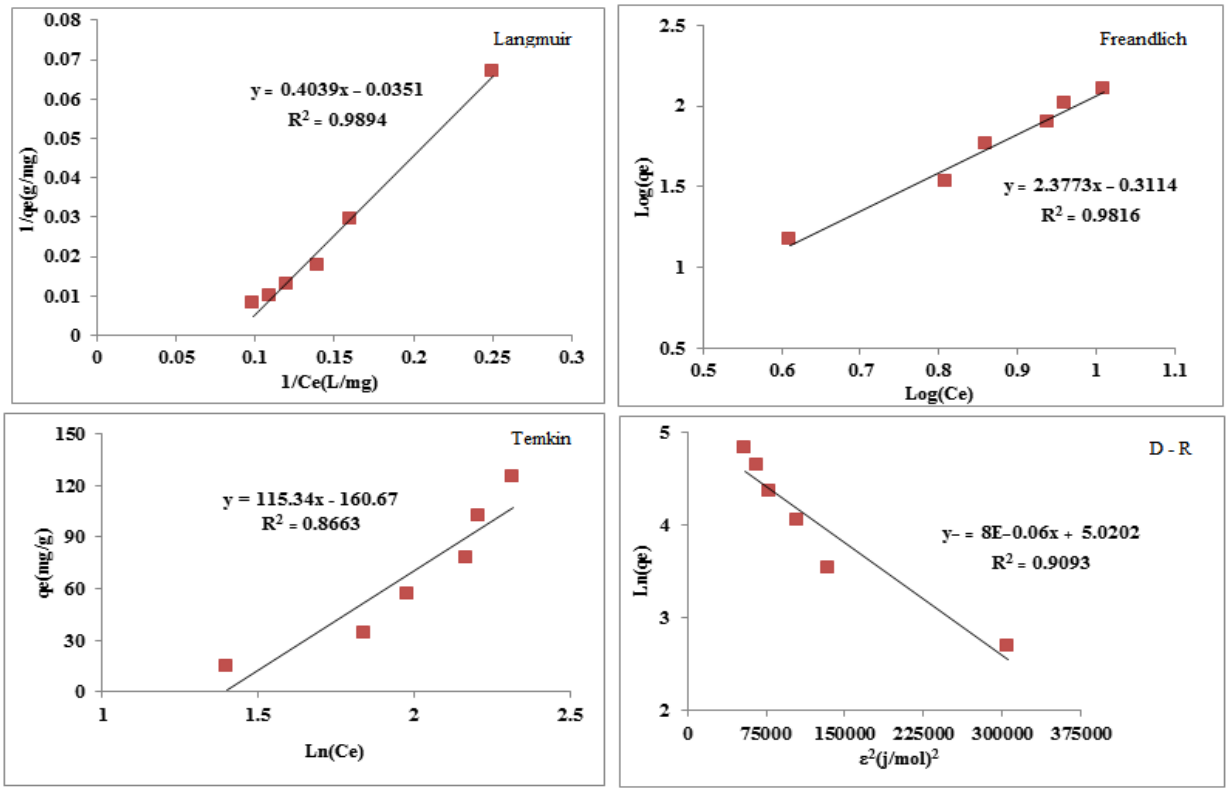

Fig. 8. Isotherm for the adsorption of Ni(II) ions onto origanum majorana-capped AgNPs. [initial Ni(II) ions conc = 30 mg L^{-1}; pH = 9.0; adsorbents dose = 40 mg; temperature = 25°C]

Table 1: Various isotherm constants and correlation coefficients calculated for the adsorption of Ni(II) ions onto origanum majorana-capped AgNPs.

Isotherm	Equation	parameters	Value of parameters For Ni^{2+}
Langmuir	$q_e=q_m bC_e/(1+bC_e)$	Q_m (mg g^{-1})	180.0
		K_L (L mg^{-1})	0.09
		R^2	0.9984
Freundlich	$\ln q_e = \ln K_F + (1/n) \ln C_e$	n	0.42
		K_F $(mg)^{1-n} L^n g^{-1}$	2.05
		R^2	0.9816
Tempkin	$q_e = B_T \ln K_T + B_T \ln C_e$	B_T	115.34
		A_T (L mg^{-1})	4.03
		R^2	0.8663
Dubinin-Radushkevich (DR)	$\ln q_e = \ln Q_d - B\varepsilon^2$	Q_d (mg g^{-1})	151.44
		$K_D \times 10^{-6}$ $(mol/J)^2$	8.0
		E (kj mol^{-1})	-247.5
		R^2	0.9093

3.8. Kinetic Study

Adsorption of a solute by a solid in aqueous solution through complex stages [35] is strongly influenced by several parameters related to the state of the solid (generally with very heterogeneous reactive surface) and to physico- chemical conditions under which the adsorption occurred. The rate of dyes adsorption onto adsorbent was fitted to traditional models like, pseudo-first, pseudo- second-order and Elovich models. The Lagergren pseudo-first order modeled scribed the adsorption kinetic data [36]. The Lagergren is commonly expressed as follows:

$$\frac{dq_t}{dt}=k_1(q_e-q_t) \quad (4)$$

where q_e an dq_t(mg/g) are the adsorption capacities at equilibrium and at time t, respectively. k_1 is the rate constant of the pseudo-first-order adsorption(L/min). The log (q_e-q_t) versus t was plotted and the values of k_1 and q_e were determined by using the slope and intercept of the line, respectively.

$$\log(q_e-q_t)= \log q_t-(\frac{k_1}{2.303})t \quad (5)$$

The fact that the intercept is not equal to q_e implies that there action is unlikely to follow the first-order. The relation ship between initial solute concentration and rate of adsorptionis linear when pore diffusion limits the adsorption process. Therefore, it is necessary to fit experimental data to another model (Table4) such as pseudo-second order model [37], based on the following equation:

$$\frac{dq_t}{dt}=k_2(q_e-q_t)^2 \quad (6)$$

Eq.(18) is integrated over the interval 0 to t for t and 0 to $q_t$for q_t, to give

$$\frac{t}{q_t}=\frac{1}{k_2 q_e^2}+\frac{t}{q_e} \quad (7)$$

As mentioned above, the plot of log (q_e-q_t) versus t does not show good results for entire sorption period, while the plot of t/q_t versus t shows a straight line. The values of k_2 and equilibrium adsorption capacity (q_e) were calculated

from the intercept and slope of the plot of t/q versus t (Table2). The calculated q_e values at different working conditions like various initial dyes concentrations and/or adsorbent masses were close to the experimental data and higher R^2 values corresponding to this model confirm its more suitability for the explanation of experimental data. This indicates that the pseudo-second-order kinetic model applies better for the adsorption of Ni(II) ions system for the entire sorption period The intraparticle diffusion equation is given as [38]:

$$q_t = k_{dif} t^{1/2} + C \quad (8)$$

where k_{dif} is the intraparticle diffusion rate constant (mg/(g. $min^{1/2}$)) and C shows the boundary layer thickness. The linear form of Elovich model is generally expressed as[39]:

$$q_t = \frac{1}{\beta}\ln(\alpha\beta) + \frac{1}{\beta}\ln t \quad (9)$$

The kinetic data from pseudo-first and pseudo-second-order adsorption kinetic models as well as the intraparticle diffusion and Elovich model are given in Table2. The linear plots of t/q_t versus t indicated a good agreement between the experimental and calculated $q_e$values for different initial dyes concentrations. Further more, the correlation coefficients of the pseudo-second-order kinetic model (R^2= 0.9831, R^2 = 0.9891) were greater than that of the pseudo-first-order model(R^2= 0.8676, R^2 = 0.99783) for Ni(II) ions respectively. As a result, respectively. As a result, the adsorption fits to the pseudo-second-order better than the pseudo-first-order kinetic model.

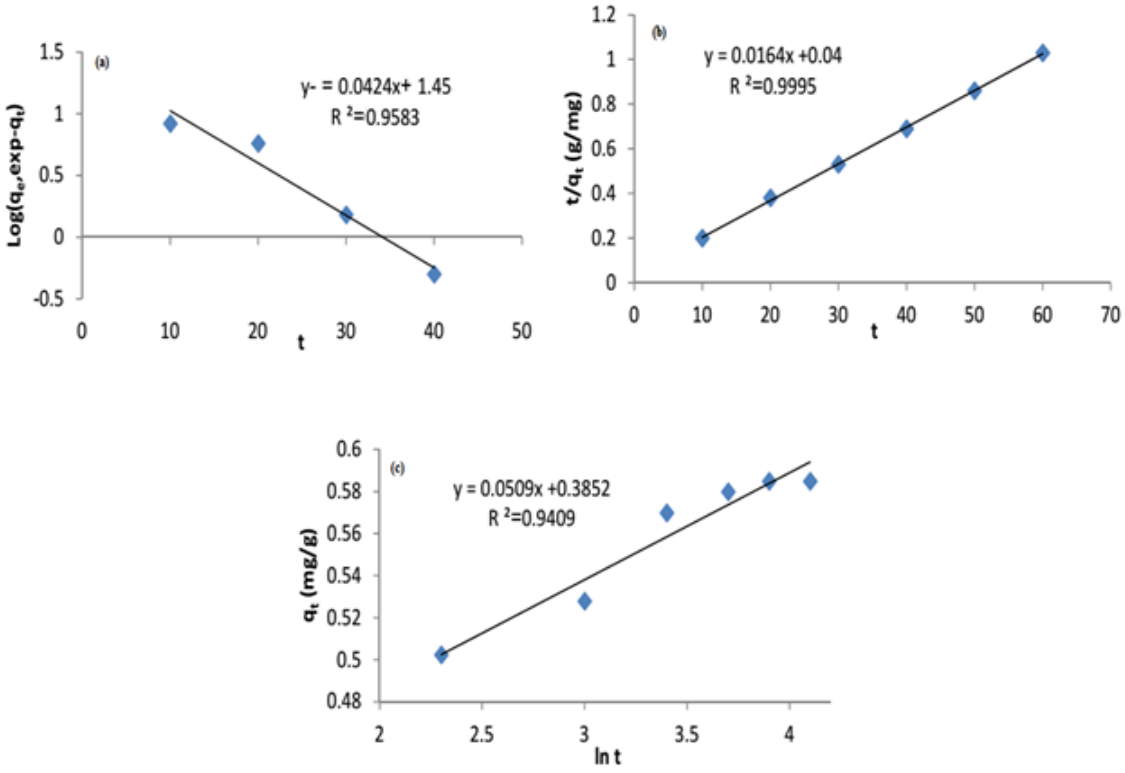

Fig. 9. Kinetic for the adsorption of Ni(II) ions onto origanum majorana-capped AgNPs. (a) pseudo-first-order kinetic model (b) pseudo-second-order kinetic model (c) intraparticle diffusion kinetic model.

Table 2: Kinetic parameters for the adsorption of Ni(II) ions onto origanum majorana-capped AgNPs.

Model	parameters	Value of parameters for Ni(II) ions
pseudo-First-order kinetic	k_1 (min^{-1})	0.1
	qe (calc) (mg g^{-1})	28.2
	R^2	0.9583
pseudo-Second-order kinetic	k_2 (min^{-1})	6.724
	q_e(calc) (mg g^{-1})	61.0
	R^2	0.9995
Elovich	β (g mg^{-1})	0.196
	α (mg g^{-1} min^{-1})	9817.42
	R^2	0.9409
q_e(exp) (mg g^{-1})		120.4

3.9. Adsorption Thermodynamics

The thermodynamic parameters, namely Gibbs free energy change (ΔG°), enthalpy change (ΔH°) and entropy change ΔS°, for the adsorption processes were determined using the following equations [40]:

$$K_c = \frac{C_A}{C_S} \quad (10)$$

$$\Delta G^\circ = -RT \ln K_{ad} \quad (11)$$

$$\ln K_{ad} \frac{\Delta H^\circ}{RT} + \frac{\Delta S^\circ}{R} \quad (12)$$

A graph (Fig. 10) is developed from a plot of lnKe against 1/T, from the slope of which ΔG can be procured. In Table.5 and 6, the summary of the thermodynamic parameter outcomes for the adsorption of Ni(II) ions onto derived origanum majorana-capped AgNPs at different temperatures is shown.

Via applying the equation adsorption of Ni(II) ions, the ΔG^o values were computed. As shown in Fig. 8, upon the increase in the temperature from 298 to 348 K, origanum majorana-capped AgNPs adsorbent diminished and therfore the exothermicity nature of the process was confirmed. The values of the thermodynamic parameters (Table 3 and 4) [41] were computed using the plots. The feasiability and spontaneity nature of the process was revealed by the negative value of ΔG^o. On the other hand, the exothermicity nature of adsorption was proven by the negative value of ΔH^o and the value of ΔS^o was a good indication of change in the randomness at the derived origanum majorana-capped AgNPs solution interface during the sorption. The fact that ΔG^o values up to -4.7 kJ/mol Ni(II) ions are accordant with electrostatic interaction between sorption sites and the Ni(II) ions (physical adsorption) has been reported. The obtained ΔG^o values in this article for Ni(II) ions are <-5 kJ/mol suggesting the predominancy of the physical adsorption mechanism in the sorption process.

3.10. Comparison of Origanum majorana-Capped AgNPs Batch Adsorption Method with Others

A comparison of the maximum adsorption capacities of different adsorbents for removal of Ni(II) ions was also reported in Table 5. The variation in qmax values between the adsorbents can be related to the type and density of active sites responsible for adsorption of metal ions from the solution. It is clear from this table that the adsorption capacity of origanum majorana-capped AgNPs used in

the present study is significant high. This may be attributed to the effect of particle size and distribution, morphology, and surface structure of the adsorbent.

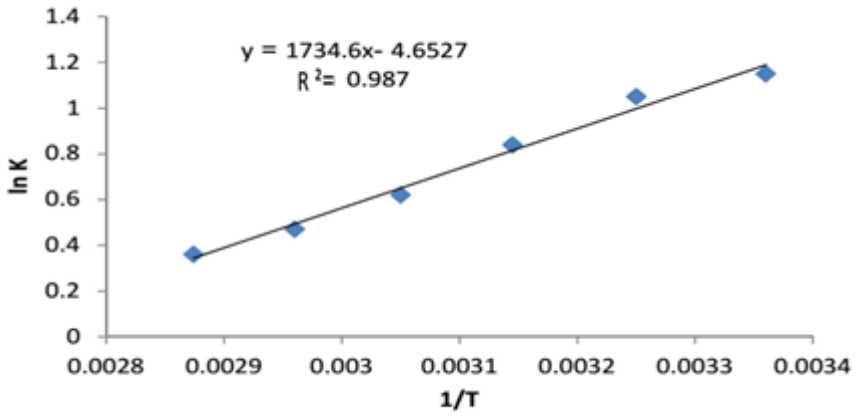

Fig. 10. Plot of ln Kc vs. 1/T for the estimation of thermodynamic parameters.

Table 3: The distribution coefficients at different temperature

ions concn. (mg/L)	R^2	K_d					
		298K	308K	318K	328K	338K	348K
Ni(II) ions 30(mg/L)	0.987	3.17	2.76	2.33	1.87	1.62	1.43

Table 4: The thermodynamic parameters for the adsorption of Ni(II) ions onto origanum majorana-capped AgNPs adsorbent

ions concn. (mg/L)	ΔH^0(kJ/mol)	ΔS^0(kJ/mol K)	ΔG^0(kJ/mol)					
			298K	308K	318K	328K	338K	348K
Ni(II) ions 30(mg/L)	-14.5	-38.7	-2.858	-2.6	-2.236	-1.706	-1.356	-1.035

Table 5: Comparison of the adsorption capacities of various adsorbents for Ni (II) removal by batch method

Metal ions	Adsorbent	Adsorption capacity (mg g^{-1})	References
		Ni (II)	
Ni (II)	pomace of olive oil factory (WPOOF)	14.80	[42]
Ni (II)	Geraphene /MnO_2	66.00	[43]
Ni (II)	Ion imprinted aniline – formaldehyde polymer	71.94	[44]
Ni (II), Co (II)	carboxylated nanoporous graphene	94.34	[45]
Ni (II), Cu (II) and Zn (II)	Sodium dodecyl sulphate coated Fe_3O_4	41.20	[46]
Ni (II), Cd (II), Pb (II) and Cr (III)	activated carbon prepared from Cucumis melo peel	23.80	[47]
Ni (II), Co (II)	Oxalate modified activated carbon	52.63	[48]
Ni (II)	origanum majorana-capped AgNPs	180.00	Present study

4. CONCLUSION

In this Study, The Origanum majorana-Capped AgNPs has been Synthesized and used as an effective adsorbent for the removal of Ni(II) ions from aqueous solutions. As a good, low-cost, and locally available adsorbent for the removal of Ni(II) ions from aqueous solutions very good. the optimum values of the pH, adsorbent dosage, Ni(II) ions concentration, and contact time were found to be 9, 40 mg, 30 mg/L, and 60 min for Ni(II) ions respectively. The effect of various process parameters showed that percent adsorption decreased with increase in initial Ni(II) ions concentration while it increased with increase in adsorbent dose. Maximum THMs removal by adsorbent was at pH 9.0. The maximum adsorption capacities (Q_m) were found to be 180.0 mg/g for Ni(II) ions respectively. Isotherm models such as Langmuir, Freundlich, Temkin, and Dubinin-Radushkevich for the adsorption process were evaluated and the equilibrium data were best described by the Langmuir model. The process kinetics was found to be successfully fitted to the pseudo-second-order kinetic model. Adsorption of Ni(II) ions was found to be spontaneous at the temperatures under investigation. The negative value of (ΔG^o, ΔH^o and ΔS^o) confirmed the sorption process was endothermic. The goal for this work is to develop inexpensive, highly available, effective Ni(II) ions adsorbents from natural waste as alternative to existing commercial adsorbents. origanum majorana-capped AgNPs has a high adsorption capacity when compared to other adsorbents for Ni(II) ions removal from an aqueous medium.

ACKNOWLEDGEMENTS

The authors gratefully acknowledge partial support of this work by the Islamic Azad University, Branch of Omidiyeh Iran.

REFERENCES

[1] H. Eccles, Treatment of metal-contaminated wastes: why select a biological process. Trends Biotechnol. 17 (1999) 462-474.

[2] G.R. Ebrahimzadeh Rajaei, H. Aghaie, K. Zare, M. Aghaie, Journal of Physical and Theoretical Chemistry. 9(3) (2012) 137-147.

[3] H. Shirkhanloo, A. Rouhollahi, H.Z. Mousavi, Journal of the Chinese Chemical Society. 57 (2010) 1035-1041.

[4] V. Obuseng, F. Nareetsile, H.M. Kwaambwa, Analytica Chimica Acta. 730 (2012) 87-92.

[5] H. Zavvar Mousavi, S.R. Seyedi, Int J Environ Sci Tech. 8 (2011) 195-202.

[6] O. Moradi, K. Zare, A.R. Zekri, A. Fakhri, Journal of Physical and Theoretical Chemistry. 9 (2) (2012) 67-76

[7] D.K. Venkata Ramana, Y. Kim, K. Kim, Indian Journal of Advances in Chemical Science. 3 (2014) 113-121.

[8] A. Khaligh, H. Zavvar Mousavi, H. Shirkhanloo, A. Rashidi, J. Applied Chem., 8 (2013) 39.

[9] C. Chen, X. Wang, Ind. Eng. Chem. Res., 45 (2006) 9144-9149.

[10] E.C. Salihi, J. Wang, D.J.L. Coleman, L. Siller. SEPARATION SCIENCE AND TECHNOLOGY. 51 (2016) 1317–1327.

[11] J. Karimi, S. Mohsenzadeh, J. Med. Sci., 64 (2013) 111.

[12] A.R. Allafchian, Z. Majidian, V. Ielbeigi, M. Tabrizchi, Anal. Bioanal. Chem., 408 (2016) 839.

[13] G.S. Dhillon, S.K. Brar, S. Kaur, M. Verma, Crit. Rev. Biotechnol. 32 (2012) 49–73 .

[14] D. Jain, H. Kumar Daima, S. Kachhwaha, S.L. Kothari, J. Nanomater Biostructures. 4 (2009) 557–563.

[15] P. Logeswari, S. Silambarasan, J. Abraham, J. Sci. Iran. 20 (2013) 1049–1054 .

[16] H. Korbekandi, S. Iravani, S. Abbasi, Crit. Rev. Biotechnol. 29 (2009) 279–306 .
[17] J.A. Dahl, B.L.S. Maddux, J.E. Hutchison, Chem. Rev. 107 (2007) 2228–2269 .
[18] J. Yan, Y. Zhou, P. Yu, L. Su, L. Mao, D. Zhang, D. Zhu, Chem. Commun. 36 (2008) 4330–4332.
[19] V.K. Gupta, O. Moradi, I. Tyagi, S. Agarwal, H. Sadegh, R.S. Ghoshekandi, A. S. H. Makhlouf, M. Goodarzi, A. Garshasbi. Environ. Sci. Technol., 46 (2016) 93-118.
[20] A.C. Burduşel, O. Gherasim, A.M. Grumezescu, L. Mogoanta, A. Ficai, E. Andronescu, Nanomaterials. 8 (2018) 681.
[21] J.S. Justin Packia Jacob, A.N. Finub, Biointerfaces. 91 (2012) 212–214.
[22] A. Sari, D. Mendil, M. Tuzen, M. Soylak, Journal of Hazardous Materials. 162 (2009) 874-879.
[23] P.K. Singh, K. Bhardwaj, P. Dubey, A. Prabhune, RSC Advances. 5 (2015) 24513-24520.
[24] [24] C. Krishnaraj, E.G. Jagan, S. Jagan, P. Rajasekar, P.T. Selvakumar, N. Kalaichelvan, Biointerfaces. 76 (2010) 50–56.
[25] G.H. Haghdoost, H. Aghaie, M. Monajjemi, Journal of Physical and Theoretical Chemistry. 13 (3) (2016) 289-296.
[26] Z. Shojaei, E. Iravani, M.A. Moosavian, Desalination and Water Treatment. 57(2016) 1-14.
[27] X. Guo, B. Du, Q. Wei, J. Yang, L. Hu, L. Yan, W. Xu, Journal of Hazardous Materials. 278 (2014) 211-220.
[28] L.F. Muhaisen, Journal of Engineering and Sustainable Development. 21 (2017) 60-72.
[29] W. Konicki, I. Pełech, E. Mijowska, Pol. J. Chem. Tech. 16 (2014) 87-94.
[30] Y.S. Ho, G. Mc Kay, Water Res. 34 (2000) 735–742.
[31] I. Langmuir, J. Am. Chem. Soc. 38 (1916) 2221–2295.
[32] Y.S. Ho, WaterRes. 40 (2006) 119 –125.
[33] R. Juang, F. Wu, R. Tseng, Environ Technol. 18 (1997) 525–531.
[34] Wood GO. Review and comparisons of D/R models of equilibrium adsorption of binary mixtures of organic vapors on activated carbons. Carbon. 40 (2002) 231–239.
[35] T. Ershad, G.H. Vatankhah, Journal of Physical and Theoretical Chemistry. 15 (1) (2018) 1-14.
[36] Y.S. Ho, "Review of Second-order Models for Adsorption Systems," Journal of Hazardous Materials, 136 (2006) 681-689.
[37] C. Namasivayam, R.T. Yamuna, Chemosphere, 30 (1995) 561-578.
[38] P.S. Kumar, K. Kirthika, J. Eng. Sci. Technol. 4 (2009) 351–363.
[39] M. Toor, B. Jin, Chem.Eng. J., 187 (2012) 79-88.
[40] R. Prabakaran, S. Arivoli, Euro. J. Appl. Eng. Sci. Res. 1(4) (2012) 134–142.
[41] G.H. Haghdoost, Journal of Physical and Theoretical Chemistry. 15 (1) (2018) 105-112.
[42] Y. Nuhoglu, E. Bioresour Technol. 100(8) (2009) 2375-2380
[43] Y. Ren, N. Yan, Q. Wen, Z. Fan, T. Wei, M. Zhang, J. Ma, CHEMICAL ENGINEERING JOURNAL. 175 (2011) 1.
[44] H. Ahmad Panahi, M. Samadi Zadeh, S. Tavangari, E. Moniri, .J. Iran. J. Chem. Chem. Eng. 31 (2012) 35-44.
[45] A. Khaligh, H. Zavvar Mousavi, A. Rashidi, Journal of Applied Chemistry. 11 (2017) 49-58.
[46] A.R. Al-Dwairi, E.A. Al-Rawajfeh, J. Univ. of Chem. Technol. and Metall. 47 (2012) 69-76.
[47] M. Manjuladevi, R. Anitha, S. Manonmani, Applide. Water. Science. 8 (2018) 36-44.
[48] Y. Saghapour, M. Aghaie, K. Zare, Journal of Physical and Theoretical Chemistry. 10 (1) (2013) 59-67.

مجله شیمی فیزیک و شیمی نظری
دانشگاه آزاد اسلامی واحد علوم و تحقیقات
جلد ۱۶، شماره ۳ و۴، پاییز و زمستان ۱۳۹۸
ISSN ۱۷۳۵-۲۱۲۶

حذف یون های نیکل (II) از محلول های آبی با استفاده از گیاه مرزنجوش پوشش داده شده با نانو ذرات نقره

زهرا کاظمی[۱] فرزانه مراحل[*۱] طوبی حموله [۲]و بیژن ممبینی گوداژدر[۳]

دانشگاه ازاد اسلامی، واحد امیدیه، گروه شیمی، امیدیه، ایران

چکیده

کاربرد سنتز جاذب گیاه مرزنجوش پوشش داده شده با نانو ذرات نقره برای حذف یون نیکل (II) از محلول‌های آبی گزارش شده است. این جاذب جدید با تکنیک های مختلفی مانند FT-IR، XRD و SEM مشخص شد. تأثیر دوز نانوذرات ، pH محلول نمونه، غلظت اولیه یون، دما، زمان تماس بین نمونه و جاذب با انجام یک روش جذب ناپیوسته مورد بررسی قرار گرفت. حداکثرغلظت اولیه یون نیکل ۳۰ میلی‌گرم در لیتر از محلول نمونه آبی، در pH برابر با عدد ۹/۰ برای یون نیکل (II) در مدت زمان ٦۰ دقیقه حاصل شد. همچنین مقدار دوز جاذب ٤۰ میلی گرم برای حذف یون نیکل (II) استفاده شد. پس از شرایط بهینه شده آزمایش حذف یون نیکل از معادله سینتیکی شبه مرتبه دوم و همچنین ایزوترم همدما از مدل لانگمویر پیروی می کند. همچنین برای به دست آوردن پارامترهای ترمودینامیکی مانند انرژی آزاد (ΔG0)، آنتالپی (ΔH0) و آنتروپی (ΔS0) از جذب استفاده شده است. مقادیر منفی (ΔG^o، ΔH^o و ΔS^o) نشان دهنده خود به خودی و گرما زا بودن روند جذب با استفاده از جاذب گیاه مرزنجوش پوشش داده شده با نانو ذره نقره برای حذف یون نیکل (II) بود. حداکثر ماکزیمم ظرفیت جذب ۱۸۰/۰ میلی گرم در گرم برای حذف یون نیکل (II) در این تحقیق حاصل گردید

کلید واژه‌ها: جذب، یون نیکل، گیاه مرزنجوش با نانوذرات نقره، ایزوترم، ترمودینامیک

[*] مسئول مکاتبات: Farzane.marahel.fm@gmail.com